Simulation and verification of hydraulic rotor gap parameters of a novel high efficient wet electro motor pump for aerospace applications

R. Tirschmann [1], D. Metzler[2], T. Koch[2], M. Spieler[1], W. Nendel[1], L. Kroll[1]

[1]TU Chemnitz, Reichenhainer Straße 31/33, 09126 Chemnitz, Germany
[2] Liebherr-Aerospace Lindenberg GmbH, Pfänderstraße 50-52, 88161 Lindenberg, Germany

Abstract

Novel Electro Motor Pump (EMP) with variable speed technology are developed for High Efficient Power Package (HEPP) solutions, which is a need for future civil aircraft platforms [5], [6]. The EMP consists out of an electronic drive and a hydraulic pump, which operates at variable rotational speeds and thus delivers variable flow rates in a wide range. The electronic drive consists out off a high efficient Permanent Magnet Synchronous Machine (PMSM) controlled from a dedicated Motor Control Electronic (MCE).

In order to increase the EMP reliability, the common shaft drive seal of legacy EMP between motor and pump, which have significant wear and reduces the EMP reliability, is eliminated by leading the hydraulic case drain flow of the hydraulic pump through the annular gap between the stator and the rotor, which is called a wet motor concept.

For optimization, it is essential to minimize the wet hydraulic rotor gap to maximize the PMSM efficiency, which causes in contrast increasing losses of the hydraulic fluid in the gap such as higher differential pressure, higher viscosity torques and higher fluid temperature. Hence, it is essential to have a clear understanding of these parameters when sizing a novel EMP for a future HEPP application.

Comprehensive simulations and tests were conducted to develop deep expertise of the hydraulic gap parameter. The simulation was verified with a lab demonstrator and adjusted based on the verification. In a second iteration, tested hydraulic pump case drain parameters and measured friction data of the motor materials were used to make a precise forecast of the hydraulic gap parameters.

Keywords: Electro motor pump, hydraulic rotor gap, HEPP, wet motor concept

1. Introduction

Novel Electro Motor Pumps (EMPs) with variable speed technology are developed for High Efficient Power Package (HEPP) solutions, which is a need for future civil aircraft platforms [5],[6]. The EMP comprises out of highly integrated hydraulic pump and an electric motor. It operates at variable rotational speeds, thus delivers variable flow rates in a wide range. The electronic drive consists out of a high efficient Permanent Magnet Synchronous Machine (PMSM) controlled from a dedicated Motor Control Electronic (MCE). State of the art legacy EMPs do have a shaft drive seal between the hydraulic pump and the dry electric motor, which has significant impact on cost and spoils EMP reliability due to wear. This shaft drive seal is now eliminated for the novel EMP in order to improve reliability and to reduce cost and complexity. It is achieved by leading the hydraulic case drain (CD) flow of the hydraulic pump directly through the annular gap between the stator and the rotor of the motor, which is called a wet motor concept.

An important constraint to be considered here is the maximum oil temperature as the hydraulic fluid produces acidity at higher temperatures, which negatively impacts the fluid characteristics the and is a stressor for all seals in the hydraulic system. The temperature in the hydraulic gap needs to be kept below 120°C for steady state condition and should not exceed 130°C for short transient conditions in order to ensure a safe and reliable pump operation.

2. Materials and Methods

2.1 Workflow Approach

The workflow approach to investigate the hydraulic gap parameters of novel high efficient wet electro motor pumps is shown in Figure 1. This illustration provides an overview of the presented work.

At first, a simplified parametric rotor-stator geometry was modeled, the so-called 1st iteration model. A parameter study was performed using this model for studying pressure drop, oil temperature and viscous torque. The results were used for the design process at Liebherr. Following, an experimental test setup was built and experimental test data recorded. To validate the simulation approach, a simulation model of the test setup was modeled. The test data is compared to the simulation results. For verification of the simulation, the roughness of the test components is measured and related to sand roughness coefficients in the simulation. This verification is the ground work for further simulation of the rotor-stator model, the so called 2nd iteration model. This model includes wall roughness and tested case drain data from a prototype pump. The results were then used to verify the final design parameters for the rotor-stator geometry of the EMP.

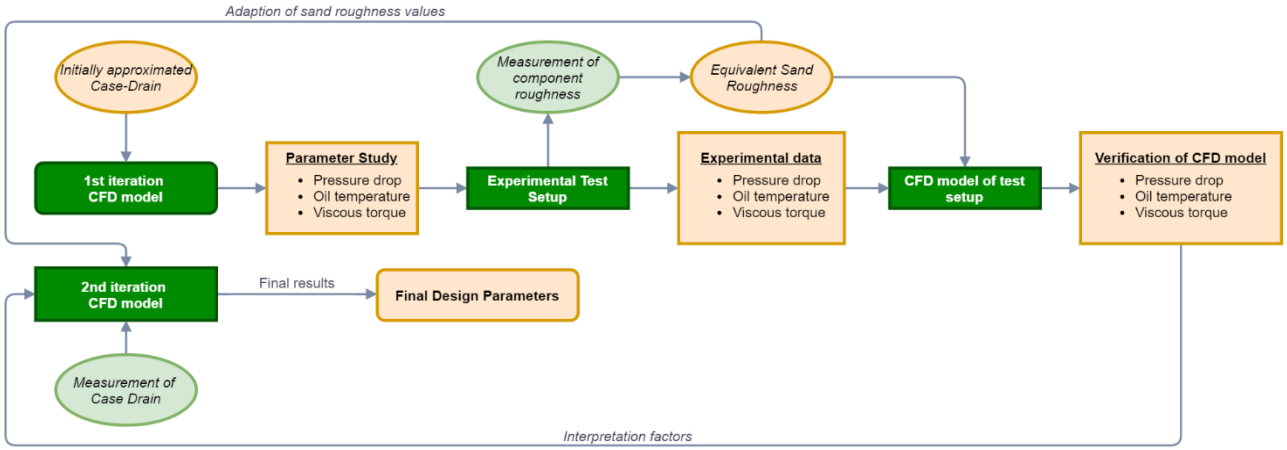

Figure 1: Workflow approach

2.2 Hydraulic Oils

Oils specified according to SAE AS 1241 are commonly used hydraulic oils in civil aviation hydraulics. The novel pump will be specified for such oils, which have a highly temperature dependent viscosity characteristic. Especially in the lower temperature range of -50°C to 0°C, SAE AS 1241 oil shows a significant temperature dependency.

An oil as per MIL-H-5606 is used for the experimental tests due to availability at the time, it has non-aggressive properties and has a similar viscosity curve for the relevant temperature range.

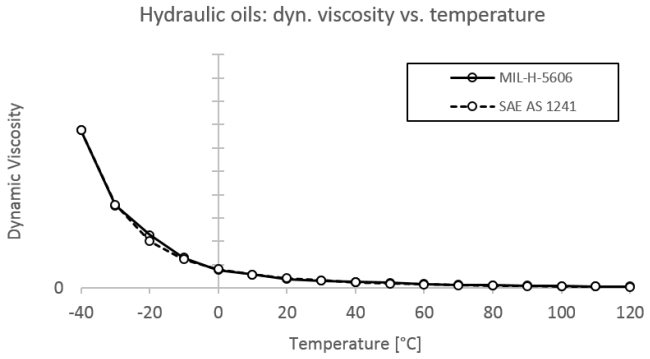

Figure 2: MIL-H-5606 and SAE AS 1241 qualitative viscosity curves used for CFD simulations [7]

2.3 Numerical models

The CFD model simulates the oil flow through the rotor stator gap. The input volume flow rate depends on the rotational speed of the pump and the oil temperature. The oil flow through the rotor gap is determined by the volumetric leakage losses of the hydraulic pump, which are described as case drain (CD) losses. Figure 3 shows the conceptual oil flow. Low Pressure (LP) oil is sucked from the hydraulic pump over the Jacket Cooling (JC) of the electric motor and the Case Drain losses are routed to external through the annual rotor gap.

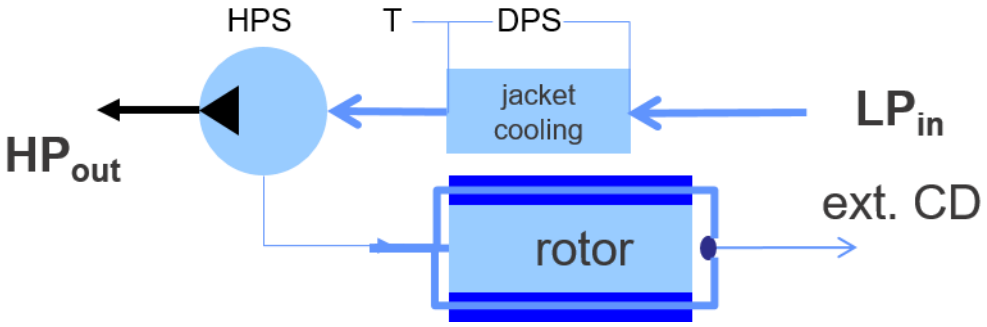

Figure 3: Oil flow through pump and rotor gap

The CD flow was calculated by Liebherr for the first iteration and later measured on a prototype pump. The corresponding CD measurement is described in the chapter 3.4. All simulations are carried out with ANSYS FLUENT software. Table 1 presents the models used for the presented results in this paper.

Table 1: Overview simulation models

Simulation ID	Boundary Conditions	Simulation Type	Description
MM1	Adiabatic walls	Steady state	Simplified motor model
TSM	Adiabatic walls	Steady state	Test setup model
MM2	Adiabatic walls, roughness	Steady state	Simplified motor model

The inlet temperature T_2 for the simulation is derived from the inlet oil temperature T_0 of the EMP. It is important to note that the temperature T_2 of the CD and thus the flow for the rotor gap is higher as the EMP oil inlet temperature T_0, see Figure 4.

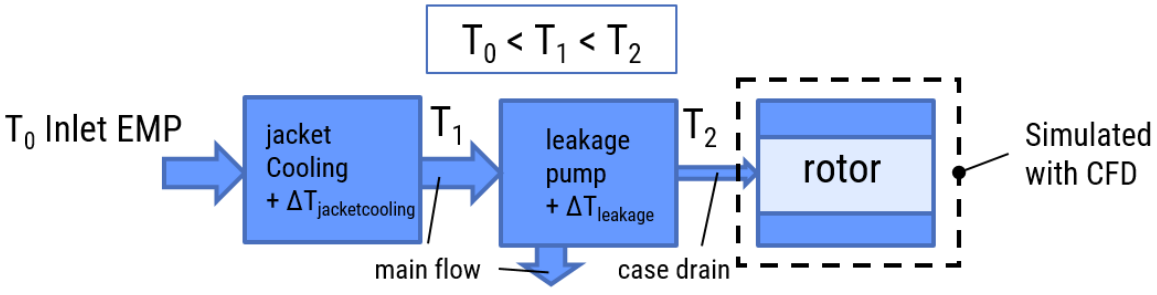

Figure 4: Inlet Temperature for rotor gap is higher than EMP inlet temperature

The oil temperature is increased from T_0 to T_1 due to heat absorption when the oil flows through the jacket cooling (JC) channels of the motor. A further temperature increase occurs from T_1 to T_2 because of the internal pressure dissipation caused from the volumetric losses within the hydraulic pump between the high pressure level and the case drain pressure level regardless of the CD flow. As a result, the inlet flow T_2 at the rotor gap relevant for the CFD simulation has always a higher temperature compared to the inlet suction temperature T_0 of the EMP.

MM1 - Motor model 1

Basic geometric parameters for the model are the gap height between rotor and stator, gap length and the rotor shaft diameter. Further input parameters are volume flow rate (case drain), inlet temperature, outlet pressure, and dynamic viscosity of SAE AS 1241 fluid. Figure 5 shows the modeled fluid volume.

The simulation uses pressure based and absolute velocity formulation. The simulations were carried out as steady state. The applied turbulence model is SST k-omega with viscous heating activated. The geometry is meshed with poly-hexcore elements. The gap area is meshed with 6 boundary layers and a minimal element thickness of appr. 0.02 mm.

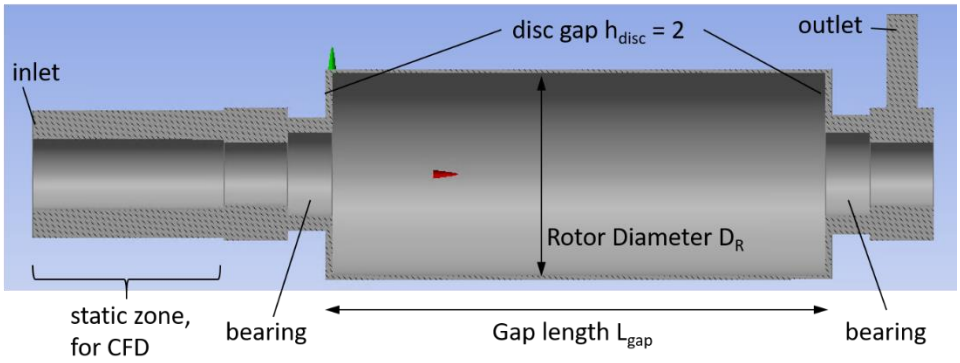

Figure 5: Fluid volume of the simplified simulation model of electric motor (geometric units in mm)

TSM1 – Test setup model

The model geometry is based on the design of the test setup rotor and stator. The viscosity model for fluid as per MIL-H-5606 as described in chapter 2.2 is used to consider the temperature dependency of oil viscosity. The solver and meshing settings are similar to the MM1 simulations.

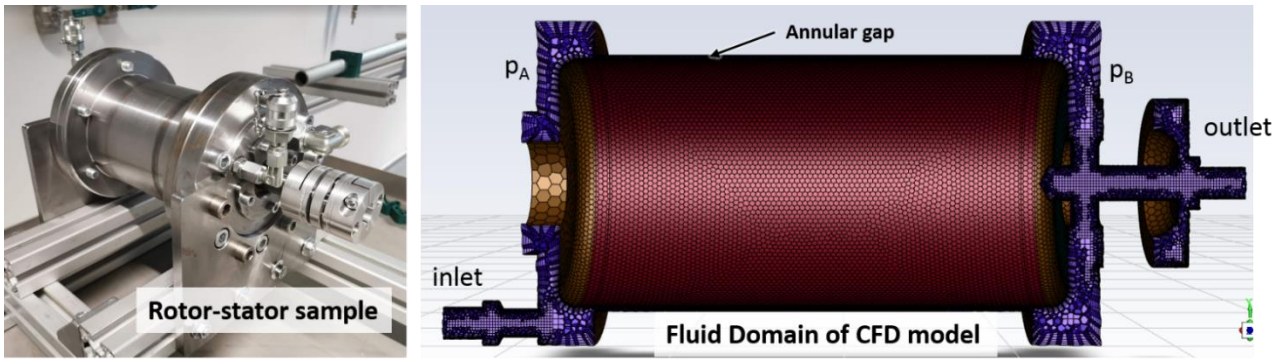

Figure 6: Modular rotor-stator test assembly and associated CFD model for simulation verification

MM2 - Motor model 2

The MM2 simulation uses the same geometric setup as MM1. Changes were made regarding wall roughness parameters and volume flow (case drain). The equivalent sand roughness values derived from the roughness measurements were implemented in the CFD model (MM2_1). Adiabatic system boundaries were assumed. The model structure, cell number and size were taken from the previous model MM1. Three temperature scenarios were considered for MM2_1, see Table 2.

Finally, the measured case drain was adopted into the model (MM2_2) and the calculations were carried out for the load case with an initial oil temperature of 104°C.

Table 2: Simulation input parameters for MM2_1

Simulation ID	speed [%]	Q [%]	T_{in} [°C]
Case 1 (Steady state)	3.7	75	104
	27.4	81	
	88.9	97	
	100.0	100	
Case 2 (steady state)	2.7	9	-1
	27.4	31	
	88.9	88	
	100.0	100	
Case 3 (transient, 0.3 s)	100.0	100	104

2.4 Experimental rotor-stator test setup

In order to investigate the temperature rise due to hydraulic friction in the gap between rotor wall and stator wall, a lab demonstrator of the rotor gap system was developed at TU Chemnitz. The hydraulic layout is set up as shown in Figure 7. The test setup consists of a pump and fluid reservoir, hydraulic fluid lines, simplified rotor stator setup with hydraulic gap, servomotor and controller, temperature, pressure and torque sensors. The DAQ system is based on Labview. Figure 8 shows the test setup as implemented at TU Chemnitz.

The rotor shaft is coupled to the servomotor shaft with a torque sensor and two flexible shaft couplings. The torque sensor measures the viscous torque due to friction between the flowing oil and the fluid enclosing walls of the rotor and stator. The temperature sensors measure the oil inlet and outlet temperatures. A differential pressure gauge measures the pressure drop between the inlet and outlet.

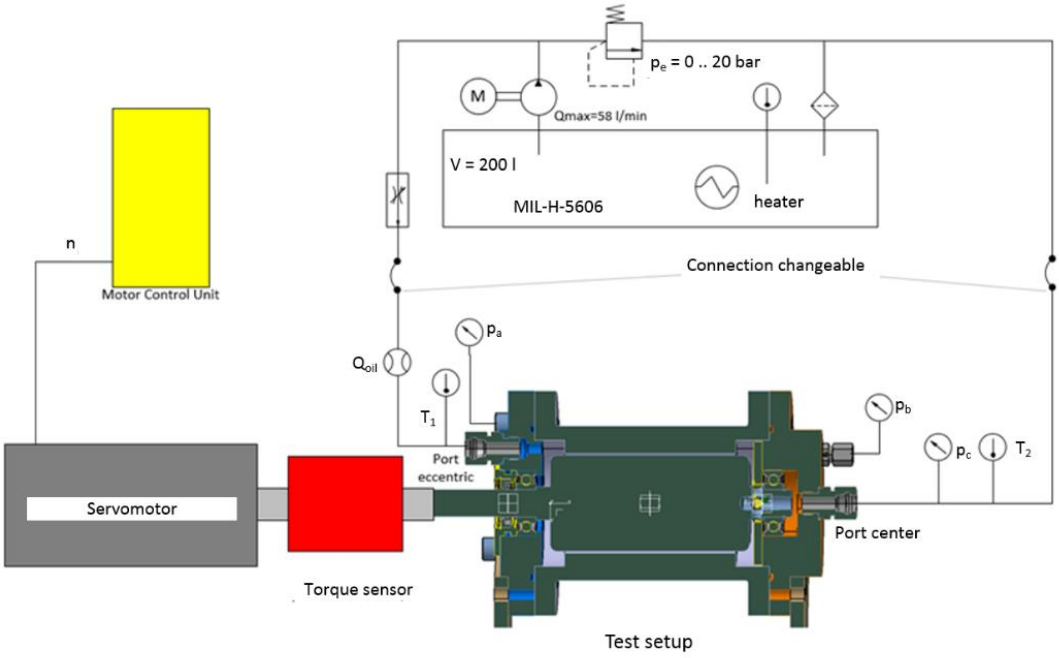

Figure 7: Hydraulic layout of test setup

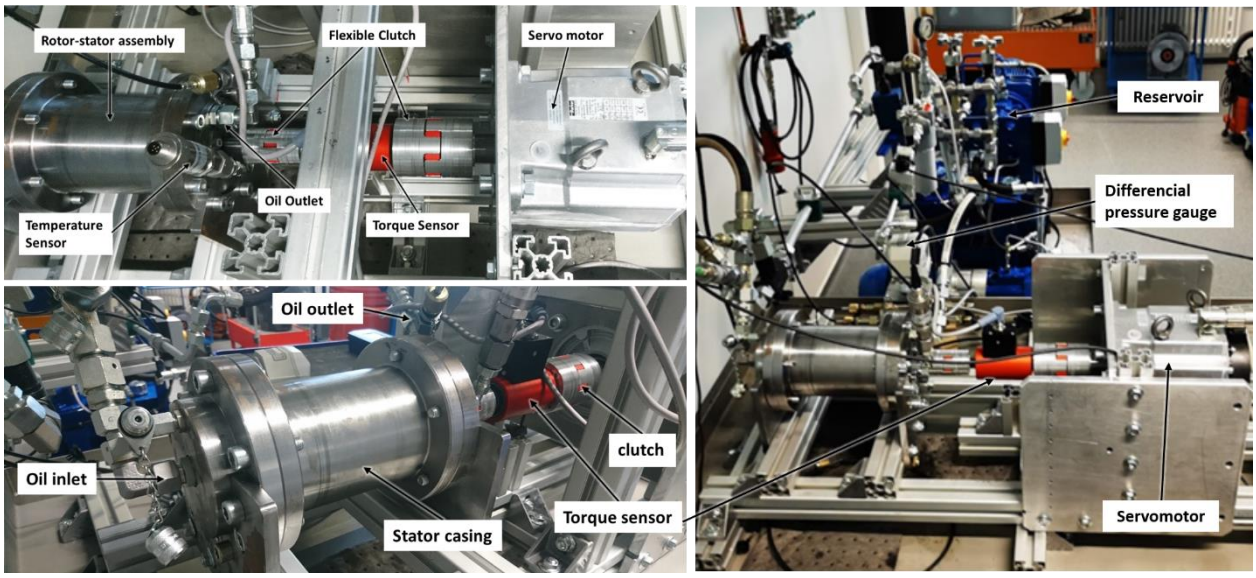

Figure 8: Lab demonstrator for verification of ANSYS FLUENT simulation

2.5. Determination of equivalent roughness coefficients for simulation

A refined simulation approach takes the roughness of the components into account. We presumed that the roughness of the walls in the motor gap influences the oil flow due to additional friction. The stator of the motor pump would be built of several stacked metal sheets. The surface of the stack, which will be in direct contact with the oil flow, would be a rough surface. The same applies to the components of the test setup. Due to machining (loathing) of the rotor shaft and stator housing, machining marks were visible and palpable. The surface roughness of the components of the test sample were measured. Measured surfaces are the lateral surface of the rotor shaft and the inner cylindrical surface of the stator housing. The roughness depth Rt is measured around the circumference and averaged, see Figure 9.

The components of interest of the motor models are the sheet stack (rotor) and the Segregation Sleeve (stator). A rough surface is expected for the sheet stack, since it is made of several stacked thin metal sheets as shown in Figure 10.

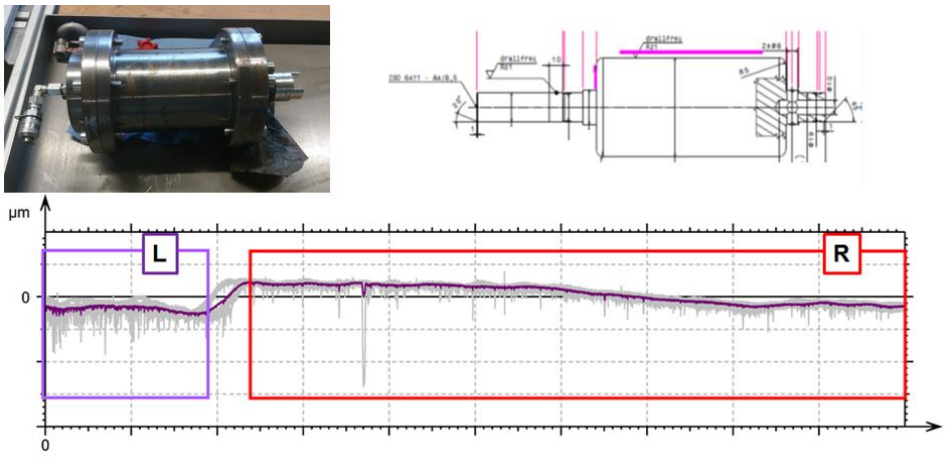

Figure 9: Exemplary measurement of rotor roughness

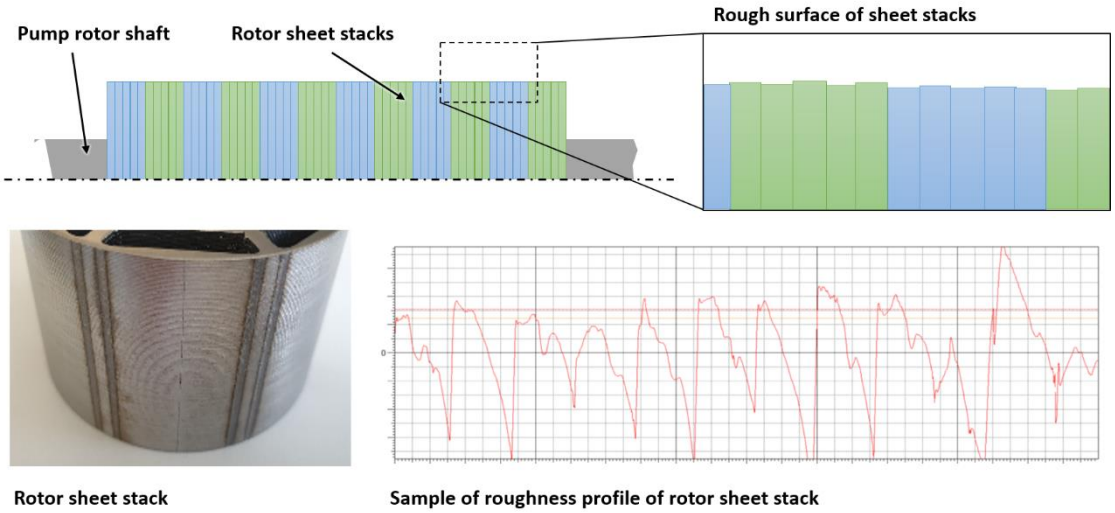

Figure 10: Rough surface of rotor sheet stack

The following two parameters define the wall roughness in ANSYS FLUENT:

(1) roughness height, K_S

(2) roughness constant, C_S

According to the ANSYS FLUENT help documentation, an 'equivalent' sand-grain roughness height could be used for K_S, if the available roughness is not a sand-grain roughness (uniform or non-uniform). The Roughness constant is set to 0.5 default. There is no clear guidance for choosing a proper value for arbitrary tapes of roughness. The standard value of C_S = 0.5 "was determined so that, when used with k –ε turbulence models it reproduces Nikurade's resistance data for pipes which are roughened with tightly-packed, uniform sand-grain roughness.", stated by FLUENT documentation [1].

The roughness height K_S is not equivalent to the technical roughness depth. K_S can be derived from the measured technical roughness either through component specific testing and parameter calibration in FLUENT or via empirical equations as described in [2] and [3]. We chose a pragmatic approach from literature, as described in the textbook Centrifugal Pumps by J. F. Gülich [3] which also accounts for machining marks from the manufacturing process. The maximum roughness depth ε_{max} relates to Rt and the arithmetic mean roughness ε_a relates to Ra. The equivalent sand roughness ε is calculated from Equation (2) or (3) [3]:

$$\varepsilon = \frac{\varepsilon_{max}}{c_{eq}} \tag{2}$$

$$\varepsilon = \frac{6\,\varepsilon_a}{c_{eq}} \tag{3}$$

Scanty information is available in the literature for the equivalence factor c_{eq}. Hein provides such values in [4]. The sand-grain roughness parameters for the FLUENT simulations were calculated according to equations (2) and (3) based on the measured roughness data.

3. Results

3.1 Initial simulation results for parameter study (MM1)

At first, a CFD model in Ansys FLUENT was developed to analyze the hydraulic gap parameters for several relevant operating points of the pump (rotary speed up to 10.000 rpm). Input parameters such as rotor speed, case drain of the pump and geometric parameters (hydraulic gap length and thickness) were considered. Initial results have shown, that the hydraulic fluid could reach critical temperatures at high rotor speeds and low volume flow rates.

Figure 11a shows the pressure drop dependent on rotor speed and for several oil temperatures. For comparison, the speed-dependent volume flow always corresponds to the same case drain rate. A dependence of this value on the temperature is neglected to illustrate the effect of temperature and rotor speed on the pressure drop. The pressure drop is defined as the difference between the inlet pressure and the outlet pressure. A positive pressure difference therefore shows a pressure drop towards the outlet. Negative pressure differences can be equated with an increase in pressure towards the outlet due to the centrifugal pumping action, which corresponds to a suction effect.

A decreasing pumping effect is observed with increasing temperature. In particular, the direction of the outlet has a large influence on the pressure drop. The rotation of the rotor creates a centrifugal pressure field that wants to push the oil outwards. According to its mode of operation, this structure acts similar to a centrifugal pump. In order to take advantage of this centrifugal effect, it is important to finally direct the oil to the outside (radial direction). For design reasons, however, it is necessary to direct the oil again in the direction of the axis of rotation after it has flowed through the straight gap between the rotor and stator in order to flow through the right-hand roller bearing. Afterwards, the oil is then directed outwards through a fixed hole.

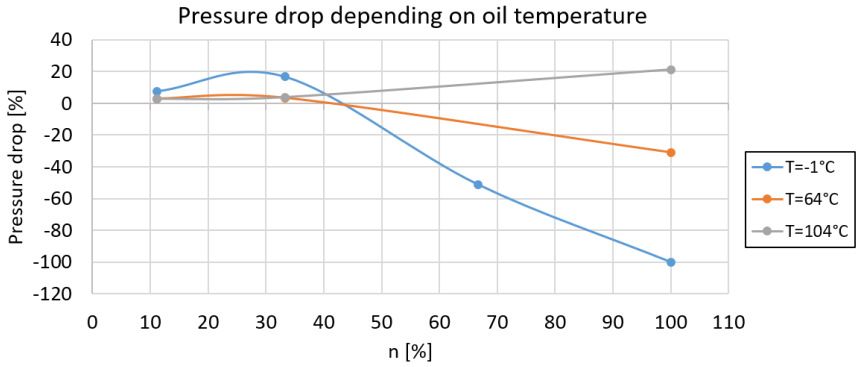

a) MM1_1: comparison of pressure drop vs. rotor speed for different oil temperatures with equivalent volume flow rate

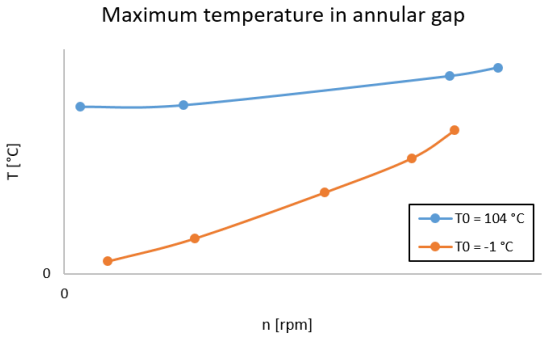

b) MM1_2: maximum gap temperature vs. rotor speed

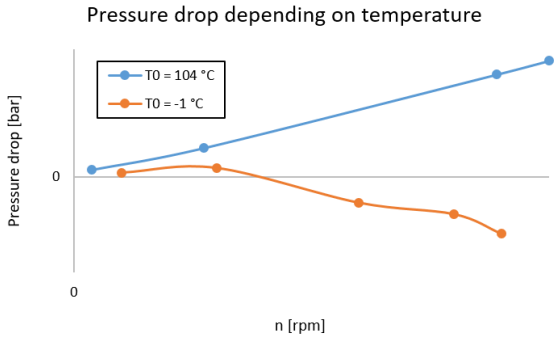

c) MM1_2: pressure drop vs. rotor speed

Figure 11: Maximum temperature and pressure drop

In Figure 11b and Figure 11c, the maximum gap temperature and pressure loss are studied. For a case drain temperature of -1°C, the maximum temperature remains below 120°C and the pressure drop is negative for high rotor speeds. A suction effect is observed. At a case drain temperature of 104 °C, the maximum temperature is in the range of 120°C. At transient maximum operation point, the maximum temperature exceeds 120°C, but stays below maximum allowed transient temperature. Delta p is positive in this temperature range, meaning a loss of pressure towards the outlet.

3.2 Experimental measurements of pressure drop, temperature and viscous torque

The developed test setup provides data for pressure drop of the oil, resulting viscous torque due to inner friction of the oil circulating through the narrow rotor-stator gap and the temperature increase. First, a baseline test was performed. The baseline establishes the rotor torque, which results from bearing and sealing friction. The measurements are performed for several rotor speeds. For each measurement at a specific rotor speed, the speed is kept constant for 30 seconds. The volume flow is set to a constant volume flow. Data shows linear progression of torque with increasing rotor speed.

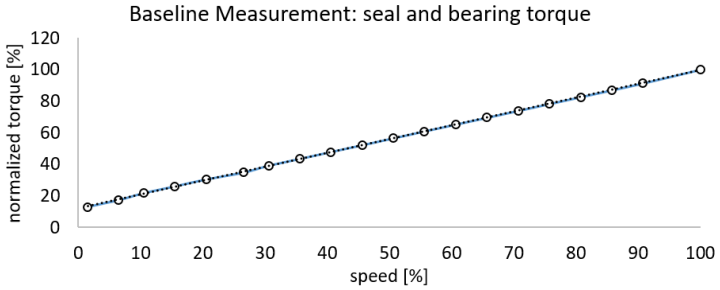

Figure 12: Normalized torque baseline data due to bearing friction

The baseline curve needs to be subtracted from any subsequent torque measurements for the actual tests. This is necessary to derive the true viscous torque due to friction between the oil flow and the static casing and rotating rotor. For further calculations, linear regression equations were derived for the baseline torque T_{ref} curves.

The viscous torque T_{vis} is calculated by substracting T_{ref} from the measured torque T_{meas}:

$$T_{vis}(n_{rotor}) = T_{meas}(n_{rotor}) - T_{ref}(n_{rotor}) \quad (4)$$

The results of two test series are presented, according to parameter sets shown in Table 3:

Table 3: Test parameter sets

Test series	Q [%]	n_{rotor} [%]
A	Steady: 100	Variable: 5 - 100
B	Variable: 32 – 100	Steady: 100

The test series A is shown in Figure 13:a. Measurement points were taken on several rotor speeds. Rotor speed was held constant for several minutes for each measurement point to achieve a steady state temperature regime (stator case and rotor temperature equals oil temperature). The reservoir is not equipped with a cooling system. The heated oil which flows back to the reservoir very slowly increased the reservoirs temperature. The viscous friction torque increased approximately linear until max speed was reached. The relative temperature difference ΔT (gray) is $(T_1 - T_0)/ T_0$. At maximum rotor speed, the max. $\Delta T = 69\ \%$ is observed. The pressure difference (right diagram, green curve) shows strong dependency on the rotor speed and reaches its maximum at max. speed.

Figure 13:b shows the results of test series B. The tests were performed at steady max. rotor speed, a and on several volume flow rates. The temperature difference ΔT increases sharply from 67 % at max. volume flow rate to 114 % at min. volume flow rate with decreasing volume flow. Due to the higher temperature, the viscosity of the oil decreases and the friction torque drops accordingly. As the volume flow increases, the pressure drop increases slightly by 3 %. Consequently, the decisive factor regarding the pressure drop is the rotor speed and not the level of the volume flow.

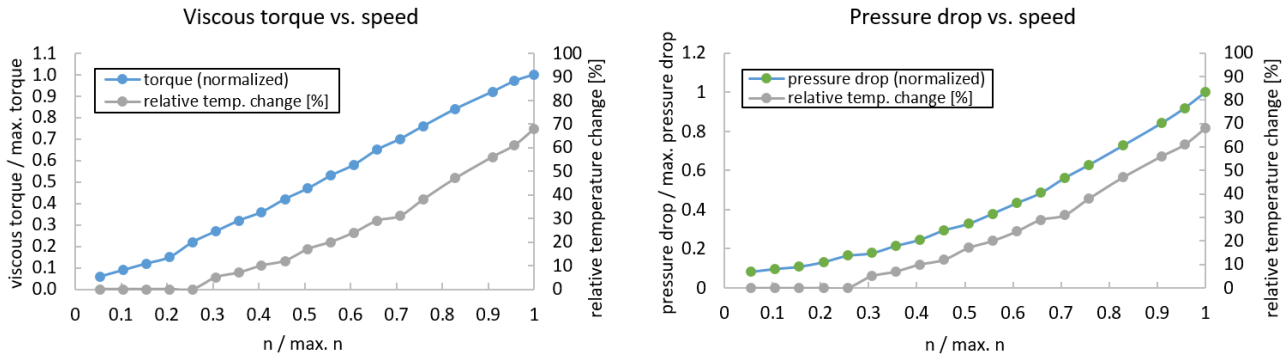

a) Test series A: Viscous torque and pressure drop vs. rotor speed for start oil temperature ; constant volume flow

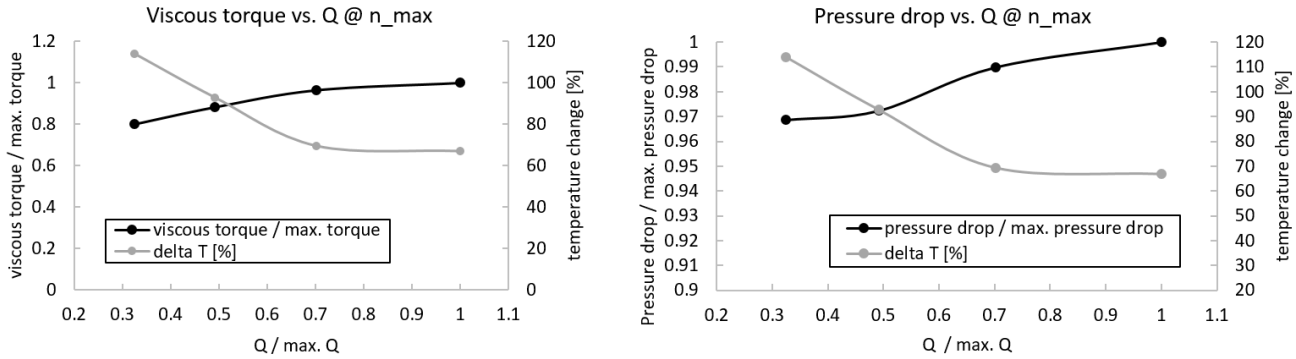

b) Tests series B: Viscous torque and pressure drop vs. oil vol. flow rate

Figure 13: Test measurements of temperature difference, pressure difference and torque vs. flow rate; a) rotor speed dependent data; b) volume flow dependent data

3.3 Verification of numerical model TSM1

For the validation of the simulation approach using real world data, the test setup was modeled in ANSYS FLUENT. The simulation results showed good approximation of the measured data with a variance on the conservative side. The simulation data and measurements of the lab model were used to deduce adjustment factors. The adjustment factors for fluid temperature, pressure difference and viscous torque are used as correction factors in order to interpret the simulation results for design purposes and sizing of new EMP.

The following figures show the simulation results for the change in oil temperature, the pressure drop and the resulting viscous torque. Results are shown for initially estimated sand-grain roughness parameters and for the roughness values derived from the roughness measurements, as described in chapter 2.5. For comparison, the test data is shown (red curves). The gray curves show the relative deviation of the simulation values from the experimental value. The relative deviation is calculated using Equation (5).

$$\frac{Value_{measured} - Value_{roughness}}{Value_{measured}} * 100\% \quad (5)$$

Figure 14: shows the measured temperature change ΔT (red curve) and the simulation results (black curves). The measured temperature change is lower than the simulations suggest for the whole rotor speed range. The maximum relative deviation occurs at max speed.

Figure 15: shows the measured pressure drop Δp (red curve) and the simulation results (black curves). The measured pressure difference is higher than the simulations suggest for the whole rotor speed range. The maximum relative deviation at max. speed is -34%.

Figure 16: shows the viscous torque (red curve) and the simulation results (black curves). The measured torque is higher than the simulations suggest for the whole rotor speed range. The maximum relative deviation at max. speed is -14 %

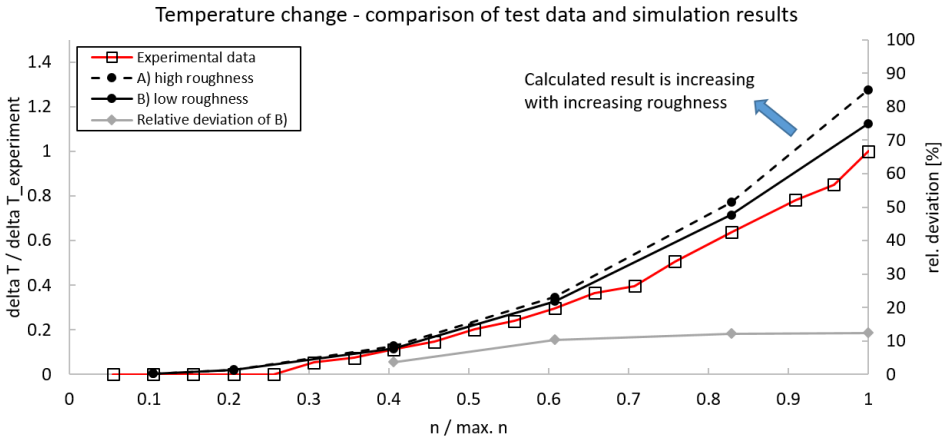

Figure 14: Temperature change ΔT with and without wall roughness

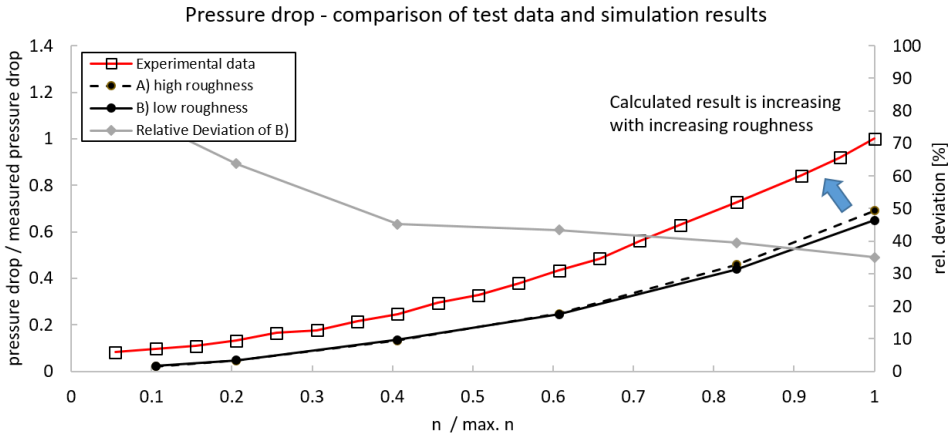

Figure 15: Pressure difference Δp with and without wall roughness

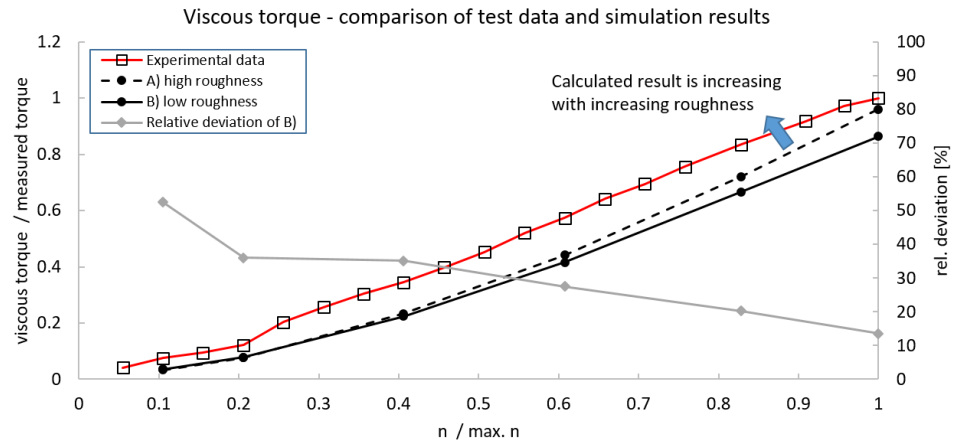

Figure 16: Viscous torque with and without wall roughness

3.4 Experimental Case Drain data

Experimental tests have been performed on a prototype EMP (see Figure 17) with a non-integrated HEPP hydraulic pump in order to characterize the external pump case drain (CD) at three different fluid temperatures. The CD flow and temperature has been measured at steady state conditions between minimum and maximum operation speed in incremental steps.

The measured case drain at low operation temperature (LT) is in good accordance with the previously calculated case drain. Since the operation at a high temperature range is regarded as the most critical oil starting temperature at the gap entrance (inlet temperature), the high temperature (HT) measurement of the CD was used for final simulation.

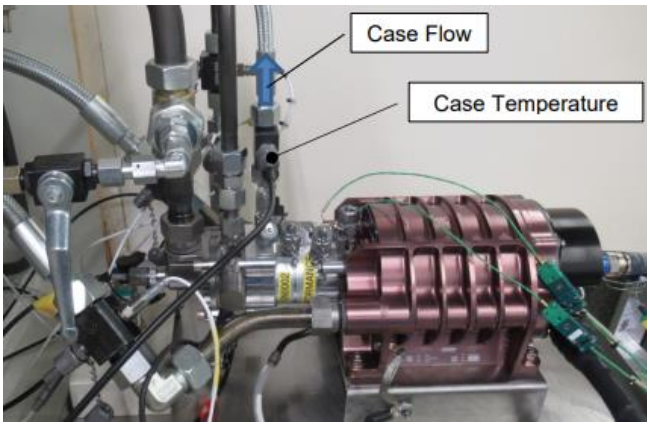

a) Case Drain Test setup

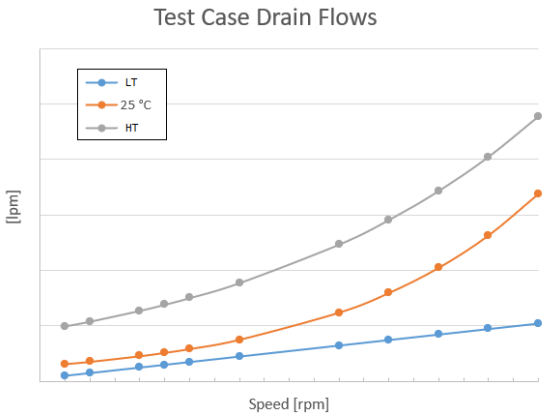

b) Test results of Case Drain Flows at different fluid temperatures

Figure 17: Case Drain test set up of an Electro Motor Pump and CD characteristics

3.5 Numerical simulation results of MM2_1 – Implemented roughness

For cases 1, 2 and 3 the results are shown in the following diagrams. The curves for the values of the previous models with the overestimated roughness (high roughness), corrected roughness (low roughness) and the hydraulically smooth model without roughness are shown for comparison.

The results of the simulation for case 1 and case 2 with the updated roughness (grey curves) show only slight deviations from the results with hydraulically smooth walls (orange curves). This applies to the maximum temperature, the pressure difference and the viscous torque, as shown in Figure 18: and Figure 19.

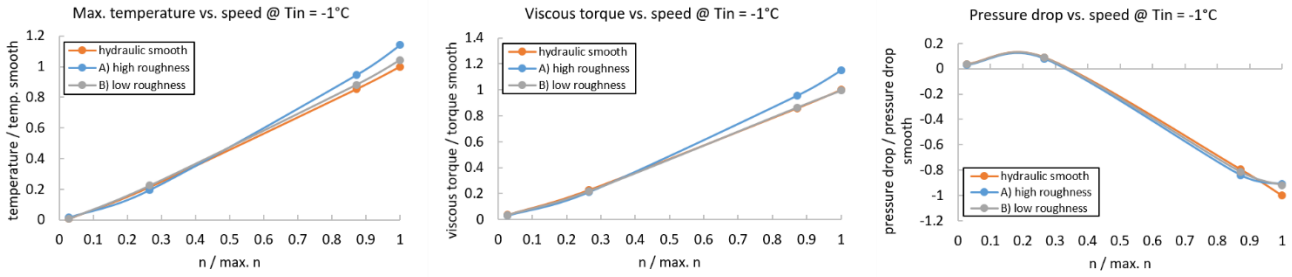

Figure 18: Results for case 1 (-1°C inlet temperature)

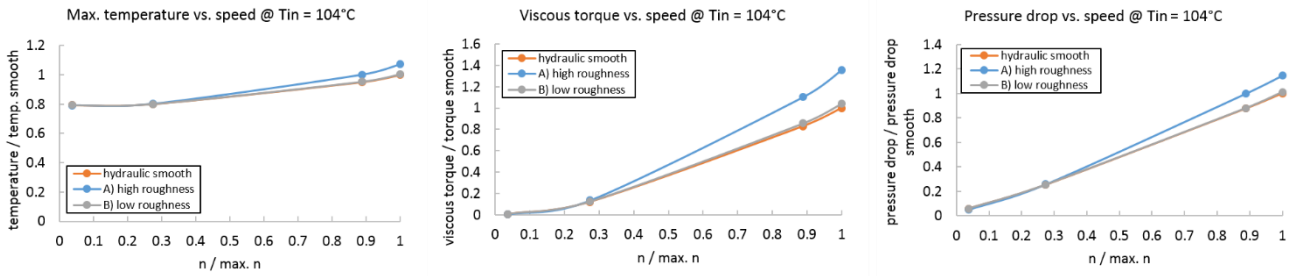

Figure 19: Results for case 2 (104°C inlet temperature)

In case 3, the transient load case, the motor pump is briefly turned up to maximum speed for 0.3 s. The resulting maximum temperature is well below the maximum temperature of the steady state simulation at the same rotor speed. Figure 20: shows the temperature curve, normalized with the max. steady state temperature from case 2.

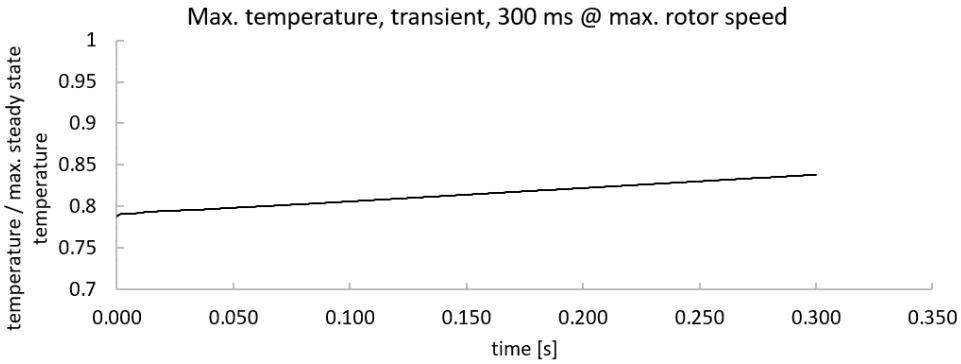

Figure 20: maximum gap temperature; transient load case 3; t = 300 ms

3.6 Final Numerical simulation results (MM2_2) – Roughness and Measured Case Drain

The speed dependent case drain at high temperature range (HT), as measured in chapter 3.4, represents the input volume flow-rate for the model MM2_2. The results in Figure 21: show a maximum gap temperature of less than 120 °C at max. rotor speed. Therefore, the maximum temperature is still in the non-critical range of below 120°C assuming static operation of the motor pump at maximum speed (steady state simulation). Compared to the results of the MM2_1 model, there is a significant reduction in the maximum temperature to < 120°C. The improved heat dissipation due to the increased volume flow in the engine gap decreases the max. temperature in the gap as expected.

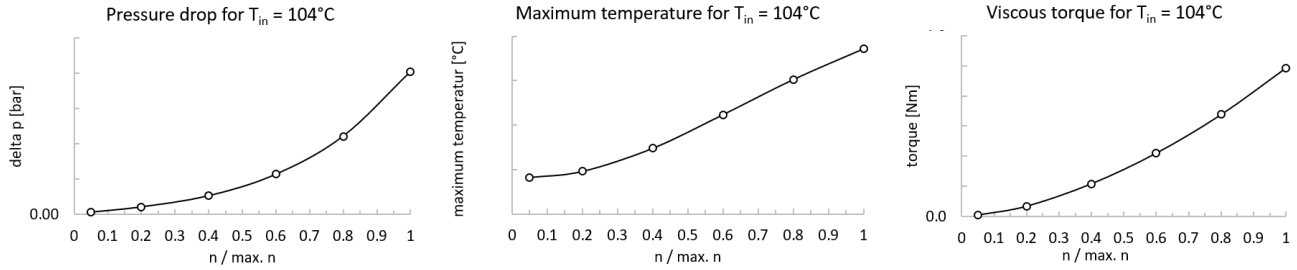

Figure 21: Results for MM2_2 with measured case drain

4. Discussion and Conclusion

4.1 Model verification and influence of wall roughness on gap parameters

The determined sand-grain roughness values (derived from the technically measured roughness) have a minor influence on the simulation results compared to the ideally smooth model. The validation of the test setup model showed:

- the temperature change is overestimated (+12 % @ max. rotor speed),
- the pressure difference is underestimated (-35% @ max. rotor speed) and
- the viscous torque is underestimated (-14% @ max. rotor speed)

The maximum temperature is the primarily relevant parameter when dimensioning the motor pump. Using the simulation results, the expected maximum temperature can be estimated conservatively. In addition to verifying the test setup model, the influence of sand-grain roughness on temperature, pressure and torque was examined using the simulation model TSM. For this purpose, a parameter study was carried out. The temperature and torque increase with increasing roughness. Using the example of sand roughness on the stator, the following findings can be summarized:

- As roughness increases, viscous torque increases slightly
- As roughness increases, the temperature difference increases slightly

4.2 Interpretation of simulation results

The results are interpreted using quality factors. The quality factors were calculated based on the relative deviations for the maximum speed. Based on this, the results of model MM2 are interpreted. The quality factors are summarized in Table 4. The factors are calculated from the relative difference between measured value and calculated value.

The following findings can be derived from the results of Table 4. The increase in temperature (temperature difference between outlet and inlet temperatures) is overestimated by 12%. The simulation result should be viewed as conservative for temperature-critical applications. The pressure difference (pressure difference between outlet and inlet) is greatly underestimated at 35%. If the pressure difference is of critical importance, an appropriate safety margin should be taken into account. The viscous torque is moderately underestimated at 14%. If the torque is of critical importance, an appropriate safety margin should be taken into account.

For final interpretation of the results, the quality factors can be applied to the results of simulation models MM2_2. Taking the quality factor into account, the max. temperature is less than 120 °C and therefore only changes slightly. The calculation results served as a dimensioning basis for LLI for the development of the EMP and the associated temperature management. With the help of the simulations the motor gap height and length could be specified. The goal of keeping the temperature below 120 °C at all operating points of the pump can be achieved.

Table 4: Quality factor for interpretation of MM2 simulation data

	Δ temperature	**Δ pressure drop**	**torque**
Relative deviation of simulation results to experimental data: *Deviation = (Experiment-Simulation)/Experiment * 100 %*	+12 %	-35 %	-14 %
Derived ‚*Quality Factor*' for interpretation of the simulation results: *QF = 1/(1+Deviation/100)*	*0.893*	*1.538*	*1.163*

4.3 Outlook

In the near future the novel HEPP EMP with a highly integrated pump and a wet motor will be commissioned. Detailed measurement will be conducted in order to verify the predicted rotor gap parameters.

5. Acknowledgements

This work was funded by the German Federal Ministry of Economic Affairs and Climate Action (BMWK) within the MODULAR project (funding code: 20Y1910G) in the national LuFo VI-1

Supported by:

Federal Ministry
for Economic Affairs
and Climate Action

on the basis of a decision
by the German Bundestag

6. Contact Author Email Address

dirk.metzler@liebherr.com

ramon.tirschmann@mb.tu-chemnitz.de

7. Copyright Statement

References

[1] ANSYS FLUENT 12.0/12.1 Documentation. www.afs.enea.it/project/neptunius/docs/fluent/. [Accessed on 2024/05/08].

[2] Adams T.and Grant C. A simple algorithm to relate measured surface roughness to equivalent sand-grain roughness. *International Journal of Mechanical Engineering and Mechatronics.* Vol. 1, Issue 1, pp 66-71, 2012.

[3] Gülich J. F. *Centrifugal Pumps.* 2rd edition, 2010.

[4] Grein H. Einige Bemerkungen über die Oberflächenrauheit der benetzten Komponenten hydraulischer Großmaschinen. *Escher Wyss Mitteilungen*. Nr. 1, pp34-40, 1975.

[5] Trochelmann N, Rave T, Thielecke F and Metzler D: An investigation of electro-hydraulic high efficient power package configurations for a more electric aircraft system architecture. In Deutscher Luft- und Raumfahrtkongress, Munich, 2017.

[6] Lima, L.Z.; Duval, M.N.; Zantner, T.; Metzler, D.; Lammering, T.; Thielecke, F.; Trochelmann, N.; Bischof, P.S.: Development of a high efficient power pack, 33rd Congress of the International Council of the Aeronautical Sciences, Stockholm, 2022

[7] SAE AIR 1362